

Research Article

Increased Cycling Performance of Li-Ion Batteries by Phosphoric Acid Modified $\text{LiNi}_{0.5}\text{Mn}_{1.5}\text{O}_4$ Cathodes in the Presence of LiBOB

Maheeka Yapa Abeywardana,¹ Nina Laszczynski,¹ Matthias Kuenzel,^{2,3} Dominic Bresser,^{2,3} Stefano Passerini,^{2,3} and Brett Lucht¹ 

¹Department of Chemistry, University of Rhode Island, Kingston, RI 02881, USA

²Helmholtz Institute Ulm (HIU), 89081 Ulm, Germany

³Karlsruhe Institute of Technology (KIT), 76021 Karlsruhe, Germany

Correspondence should be addressed to Brett Lucht; blucht@uri.edu

Received 29 April 2019; Accepted 18 June 2019; Published 4 July 2019

Academic Editor: Mohamed Mohamedi

Copyright © 2019 Maheeka Yapa Abeywardana et al. This is an open access article distributed under the Creative Commons Attribution License, which permits unrestricted use, distribution, and reproduction in any medium, provided the original work is properly cited.

$\text{LiNi}_{0.5}\text{Mn}_{1.5}\text{O}_4$ (LNMO), which has an operating voltage of 4.8 vs Li/Li^+ and a theoretical capacity of 147 mAh g^{-1} , is an interesting cathode material for advanced lithium ion batteries. However, electrolyte decomposition at the electrode can gradually decrease the capacity of the battery. In this study, the surface of the LNMO cathode has been modified with phosphoric acid (PA) to improve the capacity of the LNMO/graphite full cell. Modification of LNMO cathodes by PA is confirmed by surface analysis. Additionally, the presence of lithium bis-(oxalato) borate (LiBOB) as an electrolyte additive further enhances the performance of PA modified LNMO/graphite cells. The improved performance of PA modified cathodes and electrolytes containing LiBOB can be attributed to the suppressed Mn and Ni deposition on the anode. Elemental analysis suggests that the Mn and Ni dissolution is significantly reduced compared to unmodified LNMO/graphite cells with standard electrolyte.

1. Introduction

Since the first introduction in 1990 [1], lithium ion batteries (LIBs) have been of significant interest due to the high energy density and applicability for a wide range of applications from consumer electronics and electric vehicles (EV) [2, 3]. However, the use of LIBs is limited due to high cost, concerns related to safety, power, and energy density. Increasing the energy density and lowering the cost of LIBs is extremely important for EV applications [4, 5]. One method to increase the energy density of LIBs is to increase the operating voltage. Most commercially available batteries with layered cathode materials operate at around 4.2 V vs Li/Li^+ [6]. Nevertheless, there is significant interest in cathode materials operating at higher voltages, above 4.5 V vs Li/Li^+ , such as $\text{LiNi}_{1/3}\text{Co}_{1/3}\text{Mn}_{1/3}\text{O}_2$, $\text{LiNi}_{0.5}\text{Mn}_{1.5}\text{O}_4$ (LNMO), LiCoPO_4 , and LiNiPO_4 [7, 8]. Among these electrodes, high voltage spinel LNMO is a promising cathode material that can

operate at voltages as high as 4.8 V vs Li/Li^+ . Moreover, LNMO has no cobalt, but a rather high theoretical capacity of 147 mAh g^{-1} [9–12]. The major drawbacks of LNMO are electrolyte decomposition due to higher operating voltages and transition metal ion dissolution from trace acidic impurities in the electrolyte [13]. For example, the most commonly used electrolyte, LiPF_6 in organic solvents, is found to be unstable at higher voltages and tends to decompose at the LNMO electrode surface [9]. The Mn and Ni dissolved during the charging and discharging process travel through the electrolyte to the anode, where they are deposited, thus damaging the anode solid electrolyte interphase (SEI) [14]. The continuous reaction of the electrolyte with the electrode and transition metal ion dissolution during charging and discharging eventually leads to rapid capacity fade of the lithium ion cell [9, 15].

Several different methods have been developed to inhibit electrolyte decomposition and transition metal ion

TABLE 1: Percentage anode elemental concentrations from XPS.

	C1s [%]	O1s [%]	F1s [%]	P2p [%]
Fresh anode	86	14		
STD with LNMO	25	19	38	5
1% LiBOB with LNMO	34	34	21	2
STD with PA-modified LNMO	48	23	14	4
1% LiBOB with PA-modified LNMO	43	40	5	2

STD – Standard electrolyte

dissolution during the cycling of high voltage cathodes. One of the most promising methods is the use of electrolyte additives. An additive sacrificially reacting with the surface of the cathode to generate a passivation layer on the surface can greatly enhance the stability of the electrode and increase the overall performance of the battery [16, 17]. Previous investigations revealed that lithium bis-(oxalato) borate (LiBOB) is a good sacrificial additive which generates a stable cathode passivation layer composed of oligoborates and improves the performance of LNMO cathodes [14, 18, 19].

Another effective method of reducing the electrolyte decomposition on the surface of LNMO is to protect the surface with an inert metal oxide coating such as Al_2O_3 [20, 21]. One of the superior methods for generating thin surface coatings is using atomic layer deposition (ALD). However, ALD is not commercially practical due to the high cost associated with generating ALD coatings. Recently, Passerini and coworkers have developed a transition metal phosphate coating approach, by which the coating occurs upon the electrode slurry production by adding a small amount of phosphoric acid [22–24].

Still, however, there is significant interest in developing superior methods to mitigate electrolyte decomposition and transition metal ion dissolution from LNMO cathodes. This investigation focuses on the effect of inorganic modification (phosphoric acid modification) of LNMO cathode particles in the absence and presence of the electrolyte additive LiBOB. The surface modification significantly improves the cycling performance, which is further enhanced in the presence of LiBOB. This investigation provides a novel demonstration that a combination of surface modification and electrolyte additives can act cooperatively to improve the performance of LNMO cathodes [25].

2. Materials and Methods

Battery grade ethylene carbonate (EC), ethyl methyl carbonate (EMC), lithium hexafluorophosphate (LiPF_6), dimethyl carbonate (DMC), and LiBOB were provided from a commercial supplier with a water content of less than 50 ppm and were used as received. Nitric acid was purchased from Sigma-Aldrich. Coin cell parts, Celgard, and glass fiber separators were purchased from MTI Corp.

2.1. Electrode Preparation. Phosphoric acid (PA) modified and unmodified $\text{LiNi}_{0.5}\text{Mn}_{1.5}\text{O}_4$ electrodes containing 85% (wt.) active material, 10% (wt.) conductive carbon (Super C45), and 5% (wt.) binder (Carboxymethyl cellulose) were

fabricated as discussed in detail by Kuenzel et al. [24] In brief, binder dissolved in deionized water and conductive carbon was added to the slurry followed by active material (LNMO). For PA modification, phosphoric acid was added prior to the addition of conductive carbon. Graphite anodes were prepared with 90% (wt.) graphite, 5% (wt.) conductive carbon (Super C65 and SFG6), and 5% (wt.) binder (Styrene-Butadiene Rubber/Carboxymethyl cellulose). The thickness of the anode coating was controlled to balance the LNMO and graphite electrodes with an anode to cathode capacity (n/p) ratio of 1.1-1.3.

2.2. Preparation of Coin Cells. LNMO/graphite coin cells for electrochemical performance investigations were assembled in an argon filled glove-box in duplicate with a trilayer polypropylene/polyethylene (PP/PE/PP) separator (Celgard) and a glass fiber separator. 100 μL of 1.0M LiPF_6 in EC/EMC (ethylene carbonate/ethyl methyl carbonate; 3/7, w/w) with and without 1% LiBOB (w/w) was used as the electrolyte. Assembled cells were cycled at room temperature between 3.5 V and 4.8 V with an Arbin battery cycler as it follows: C/20 first cycle; C/10 second and third cycles; C/5 for the remaining cycles for a total of 56 cycles.

2.3. Electrochemical Measurements. Princeton Instruments (V3) was used to perform electrochemical impedance spectroscopy (EIS) on the coin cells after formation cycles and 56 cycles. State of charge was 0% for all the tested cells since they were at the discharged state. The perturbation was 1 mV with the frequency range from 300 kHz to 10 mHz.

2.4. Surface Characteristics and Composition Analysis. The cathodes and anodes of the cycled cells were harvested in an argon filled glove-box. Cells were disassembled and washed with anhydrous dimethyl carbonate (DMC) three times to remove residual electrolyte, followed by vacuum drying at room temperature overnight. The electrodes were transferred to the X-ray photoelectron spectroscopy (XPS) chamber via an air free transfer vessel. A PHI 5500 system with Al $K\alpha$ radiation ($h\nu = 1486.6\text{ eV}$) under ultrahigh vacuum conditions was used for the measurements. The final adjustments were done referring to C-C of C1s at 284.5 eV. The percentage elemental concentrations in Tables 1 and 2 were calculated using following equation:

$$\text{Elemental concentration \%} = \frac{\text{Normalised peak area of element of interest}}{\text{Sum of normalized peak areas of all elements}} \times 100 \quad (1)$$

TABLE 2: Percentage cathode elemental concentrations from XPS.

	C1s [%]	O1s [%]	F1s [%]	P2p [%]
Fresh unmodified LNMO	53	39	< 1	< 1
STD with LNMO	36	34	12	4
1% LiBOB with LNMO	45	42	3	2
Fresh PA-modified LNMO	47	39	< 1	2
STD with PA-modified LNMO	46	31	9	2
1% LiBOB with PA-modified LNMO	32	60	2	1

STD – Standard electrolyte

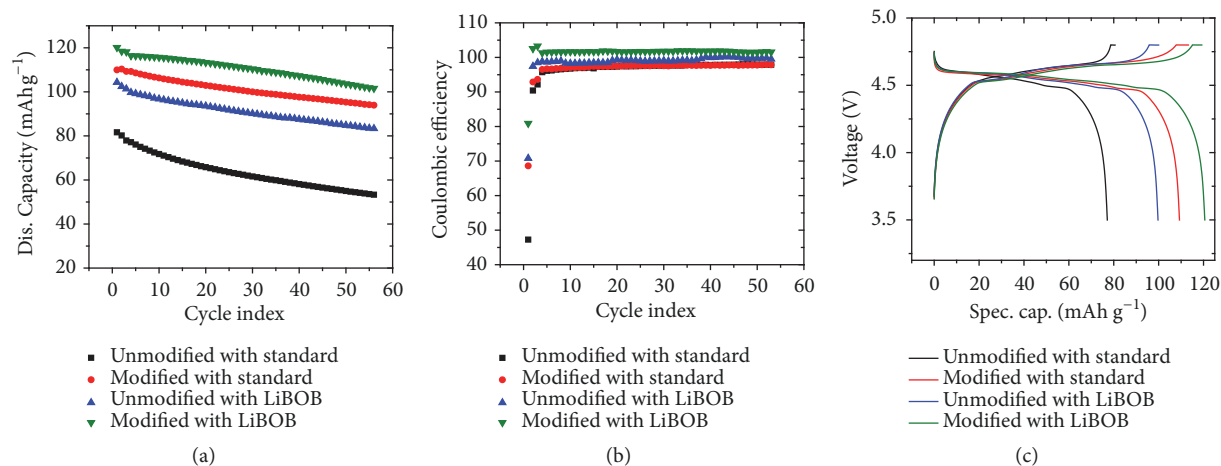


FIGURE 1: Comparison of (a) discharging capacities (based on the cathode active material), (b) coulombic efficiencies, and (c) 4th cycle charge/discharge curves of phosphoric acid modified and unmodified LNMO/graphite full cells with and without LiBOB in 1.0 M LiPF₆ EC/EMC 3/7 (w/w).

2.5. Metal Ion Dissolution Analysis. Deposition of metal ions on the anode was identified and quantified by inductively coupled plasma-mass spectroscopy (ICP-MS). Cycled coin cells were disassembled and the recovered anodes were rinsed with DMC to remove any residual electrolytes. Then 2% HNO₃ was added to dissolve the residual solids and diluted to 10.00 mL. After sonication these solutions were left for digestion for 48 h and filtered before ICP-MS analysis.

3. Results and Discussion

3.1. Cycling Performance of LNMO/Graphite Full Cells. The discharging capacities and the coulombic efficiencies were calculated from the electrochemical cycling data. A comparison of cycling performance of phosphoric acid (PA) modified and unmodified LNMO/graphite cells cycled with standard electrolyte and electrolyte with added LiBOB (1 wt.%) at 25°C is provided in Figure 1(a) and the coulombic efficiencies (CEs) of the cells are provided in Figure 1(b). Starting from the first discharge capacity there is a large improvement in the cells with PA modified electrodes. The first discharge capacity for unmodified LNMO with standard electrolyte is calculated to be 81.6 mAh g⁻¹. The battery with the PA modified electrode with the standard electrolyte displays a capacity of 110 mAh g⁻¹. This is an increase of 27.8% in discharge

capacity. The performance of unmodified and PA modified electrodes has also been investigated in the presence of LiBOB electrolyte additive. The first discharging capacity increases up to 104.3 mAh g⁻¹ and 120.1 mAh g⁻¹, respectively. For the latter, this is a significant increase compared to the unmodified electrode with the standard electrolyte, i.e., an increase of the discharge capacity by 47.2% and about 10 mAh g⁻¹ more compared to the PA modified electrode with the standard electrolyte (110.0 mAh g⁻¹). The unmodified LNMO electrodes cycled with the standard electrolyte have a first cycle CE of 47.3% whereas modified cells with standard electrolyte have a first cycle CE of 68.6%. The addition of LiBOB to cells containing both the PA modified and unmodified LNMO provides, moreover, a significant improvement in Coulombic efficiency, which is above 80% for the PA modified electrodes in the first cycle and subsequently stabilizing near 100% (Figure 1(b)). The charge/discharge curves for the cycle (4th cycle) after the formation cycles for LNMO/graphite full cells are depicted in Figure 1(c). These curves clearly show the increase in both charging and discharging capacities of the PA modified cells as well as the LiBOB added cells. The reversibility of PA modified cells are higher compared to unmodified cells and the reversibility of PA modified cells further increases with the addition of LiBOB electrolyte additive.

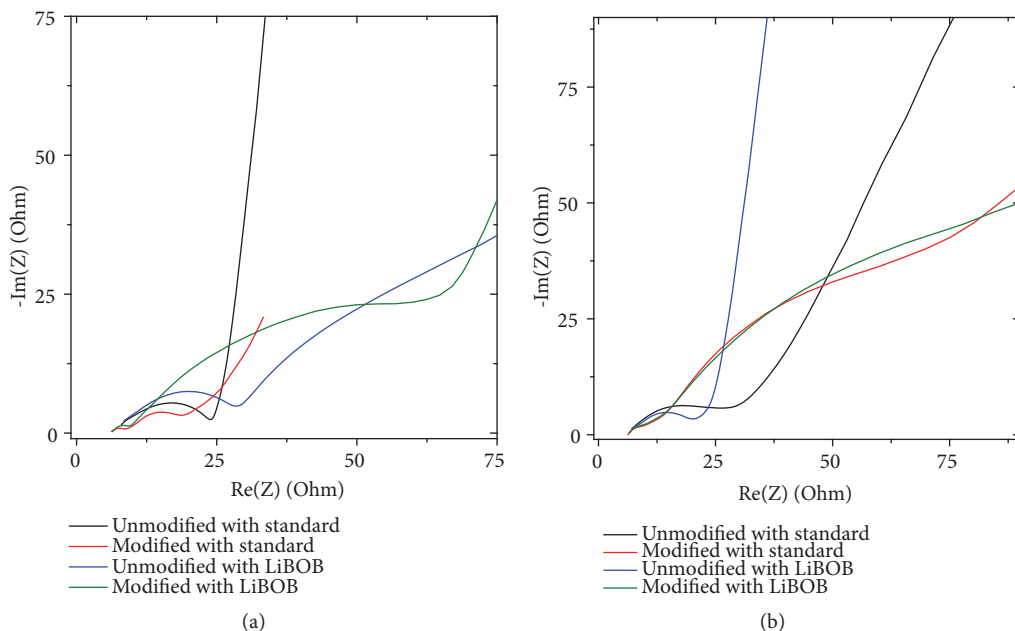


FIGURE 2: Impedance measurements of PA modified and unmodified LNMO electrodes in graphite full cells with and without LiBOB (a) after the formation cycle and (b) after 56 cycles.

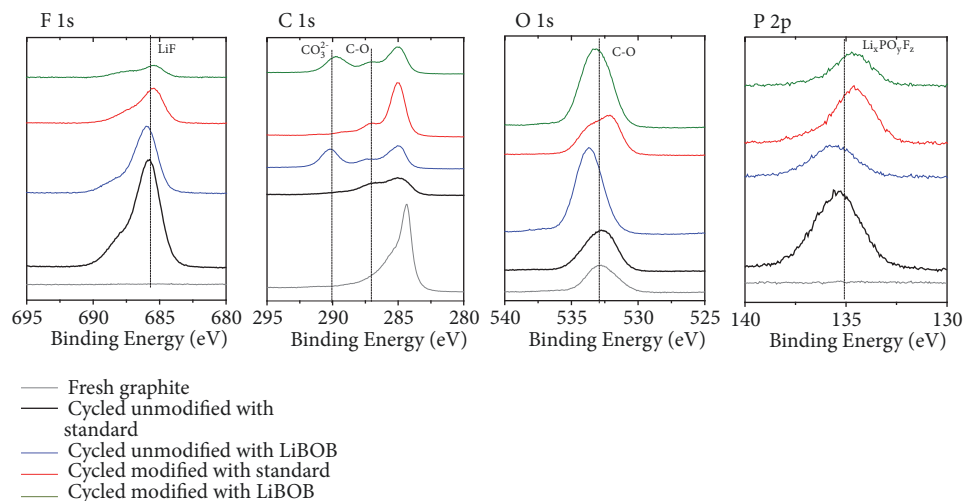


FIGURE 3: XPS surface analysis of fresh and cycled graphite in PA modified and unmodified LNMO electrodes in graphite full cells with and without LiBOB in the electrolyte.

3.2. Impedance Measurements of the Cells. To further test the electrochemical performance of the cells and to observe the impedance change over time, EIS measurements were performed. EIS of PA modified and unmodified LNMO/graphite full cells with and without LiBOB in the electrolyte (a) after the first formation cycle and (b) after 56 cycles are provided in Figure 2. The EIS spectra show that after the first formation cycle the impedance of the batteries with standard electrolyte is lower compared to the batteries with LiBOB in the electrolyte (Figure 2(a)). However, after all 56 cycles the situation is reversed and the impedance of the batteries with standard electrolyte is higher compared to the LiBOB added batteries (Figure 2(b)). During the formation cycle,

LiBOB decomposes on the positive electrode to generate a surface film with oligoborates on it [14, 26, 27]. The increase in impedance of batteries with LiBOB after the first cycle can be attributed to this surface layer. EIS of the batteries with phosphoric acid modified LNMO display lower impedance compared to unmodified LNMO, consistent with the higher discharge capacities observed for the cells with PA modified LNMO cathodes.

3.3. Surface Analysis of Anodes and Cathodes. XPS spectra of anodes obtained from cycled batteries (Figure 3) provide additional information on the composition of the surface films formed on the electrodes in presence or absence of

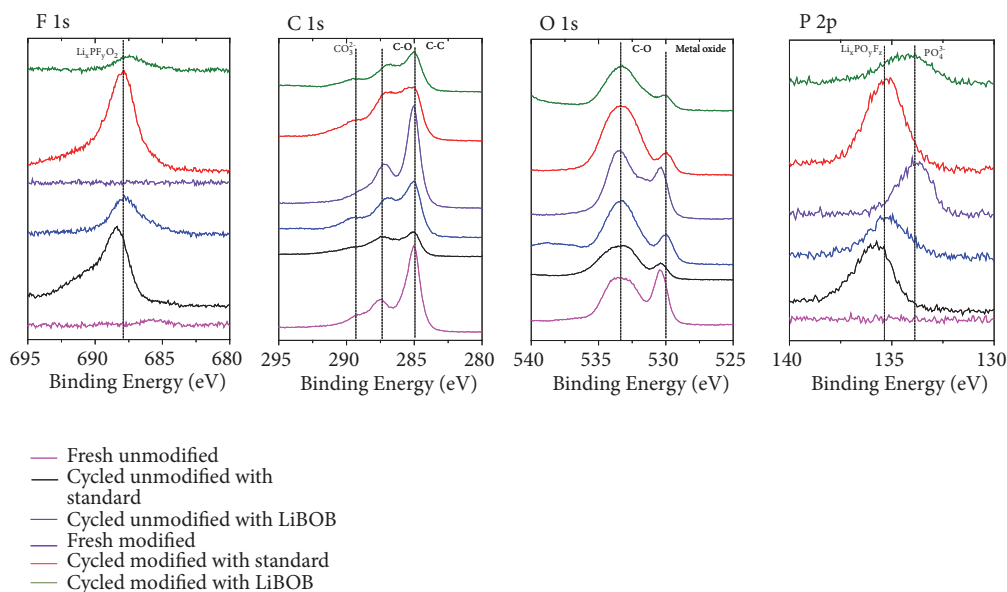


FIGURE 4: XPS surface analysis of fresh and cycled LNMO in PA modified and unmodified LNMO electrodes in graphite full cells with and without LiBOB in the electrolyte.

LiBOB and also the effect of the PA modification. The F1s spectra for anodes indicate that the intensity of the LiF peak is decreased for anodes extracted from cells containing PA modified cathodes and the intensity is further reduced with the addition of LiBOB to the electrolyte (Table 1). This is consistent with surface coated LNMO inhibiting LiPF_6 decomposition [28]. The C1s XPS spectra of the cycled anodes contain peaks at 286.8 and 290.3 eV corresponding to C-O and CO_3^{2-} consistent with the generation of Li_2CO_3 and lithium alkyl carbonates in the SEI [29]. The intensities of the C-O peak at 286.8 eV in C1s and the C-O peak at 533.0 eV in O1s are higher when LiBOB is present in the electrolyte consistent with the generation of a passivation layer containing LiBOB reduction products [28, 30].

XPS elemental spectra obtained for the (cycled) cathodes are provided in Figure 4. The presence of phosphorus on the surface is supported by the P2p spectra of the fresh electrodes, which contain a peak at 134.0 eV characteristic of metal phosphate (e.g., lithium, manganese, or nickel phosphate). In the C1s spectra C-C peak intensities of cycled electrodes are much lower compared to the fresh electrodes (see also Table 2), which is assigned to the presence of a surface film on the cycled electrodes. The peak at 688.0 eV in F1s supports the presence of $\text{Li}_x\text{PF}_y\text{O}_z$ (the binder for LNMO is not PVDF) in the surface film. The intensity of the peak is reduced in the presence of LiBOB (see also Table 2 for the quantitative analysis). This is attributed to a reduced LiPF_6 decomposition in the presence of LiBOB. The intensity of the metal oxide peak at 529.5 eV in O1s is reduced after cycling. The intensity of the metal oxide peak is higher for the fresh electrodes, further supporting the formation of a surface film during cycling. XPS data (mainly F1s) suggests that the phosphoric acid modification suppresses the

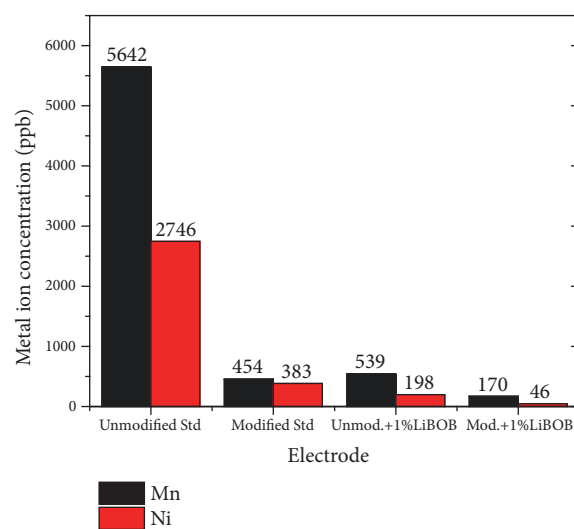


FIGURE 5: Mn and Ni concentrations in the anode electrodes of the cycled full cells, as from ICP-MS analysis.

decomposition of the electrolyte on the surface of the electrodes.

3.4. Metal Ion Dissolution. A common problem for LNMO cathodes is the transition metal ion dissolution during cycling. ICP-MS of the cycled anodes was conducted to quantify transition metal ion dissolution in cycled cells. The ICP-MS data from the cycled LNMO/graphite full cells is provided in Figure 5. The Mn and Ni concentrations for the cells with unmodified LNMO with standard electrolyte are found to be 5642 ppb and 2746 ppb, respectively. These

are the highest transition metal concentrations observed for all four types of cells, suggesting that transition metal ion dissolution is higher for unmodified electrodes with standard electrolyte. Addition of LiBOB to the cells containing the unmodified LNMO suppresses Mn and Ni dissolution by a factor of 10 and 14, respectively (Mn 454 ppb and Ni 383 ppb). The Mn and Ni concentrations for anodes extracted from the cells containing the PA modified electrodes and the standard electrolyte are 539 and 198 ppb, respectively. Also a significant reduction is compared to unmodified LNMO cells with standard electrolyte. Finally, PA modified LNMO in the presence of LiBOB shows the highest reduction in transition metal ion dissolution (Mn 170 ppb and Ni 46 ppb). Anodes containing both modified cathode and LiBOB reduce the Mn and Ni dissolution by a factor of 33 and 59, respectively. This trend in reduction of transition metal ion dissolution is in agreement with the trend in discharge capacity retention of the LNMO/graphite full cells (Figure 1(a)); i.e., the reduction of metal ion dissolution substantially contributes to the improved cycling performance.

4. Conclusions

The cycling performance of phosphoric acid modified and unmodified LNMO/graphite full cells with standard electrolyte with and without LiBOB has been investigated. The cycled cells exhibited enhanced performance upon phosphoric acid modification as well as the addition of LiBOB. The cells with LiBOB also displayed a better Coulombic efficiency.

Ex situ surface analysis of harvested cathodes and anodes has been conducted with XPS and ICP-MS. The surface film formed in the presence of LiBOB suppresses the decomposition of LiPF_6 . Phosphoric acid modification of LNMO electrodes drastically reduces the transition metal ion deposition on anodes during the cycling and the surface film formed by the decomposition of LiBOB further suppresses the transition metal ion deposition. The increased cycling performance of LNMO/graphite full cells can be attributed to the reduced transition metal ion dissolution in the electrolyte and deposition on anode due to phosphoric acid modification of the cathode and presence of LiBOB in the electrolyte.

Data Availability

All the data used to support the findings of this study are included within the article.

Disclosure

Some of the results in this manuscript have been published as the M.S. Thesis of Maheeka Yapa Abeywardana at the University of Rhode Island.

Conflicts of Interest

The authors declare no conflicts of interest.

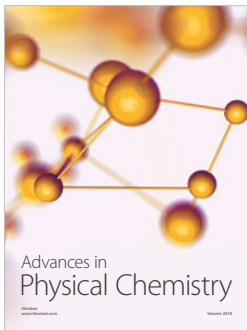
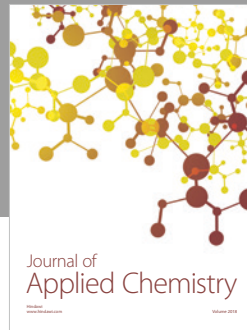
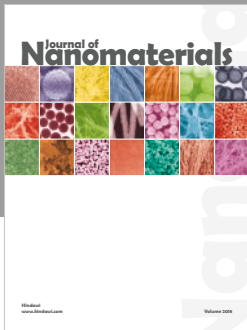
Acknowledgments

The authors Maheeka Yapa Abeywardana, Nina Laszczynski, and Brett L. Lucht acknowledge the support of Department of Energy-Established Program to Stimulate Competitive Research (DOE-EPSCoR). Matthias Kuenzel, Dominic Bresser, and Stefano Passerini acknowledge the support of the German Federal Ministry of Education and Research (BMBF) within the Li-EcoSafe project [03X4636D] and the basic support of the Helmholtz Association.

References

- [1] S. Patoux, L. Daniel, C. Bourbon et al., "High voltage spinel oxides for Li-ion batteries: from the material research to the application," *Journal of Power Sources*, vol. 189, no. 1, pp. 344–352, 2009.
- [2] B. Dunn, H. Kamath, and J. M. Tarascon, "Electrical energy storage for the grid: a battery of choices," *Science*, vol. 334, no. 6058, pp. 928–935, 2011.
- [3] M. Armand and J. M. Tarascon, "Building better batteries," *Nature*, vol. 451, no. 7179, pp. 652–657, 2008.
- [4] P. Axmann, G. Gabrielli, and M. Wohlfahrt-Mehrens, "Tailoring high-voltage and high-performance $\text{LiNi}_{0.5}\text{Mn}_{1.5}\text{O}_4$ cathode material for high energy lithium-ion batteries," *Journal of Power Sources*, vol. 301, pp. 151–159, 2016.
- [5] D. Hong, Y. Guo, H. Wang, J. Zhou, and H. Fang, "Mechanism for improving the cycle performance of $\text{LiNi}_{0.5}\text{Mn}_{1.5}\text{O}_4$ by RuO_2 surface modification and increasing discharge cut-off potentials," *Journal of Materials Chemistry A*, vol. 3, no. 30, pp. 15457–15465, 2015.
- [6] B. L. Ellis, K. T. Lee, and L. F. Nazar, "Positive electrode materials for Li-Ion and Li-batteries," *Chemistry of Materials*, vol. 22, no. 3, pp. 691–714, 2010.
- [7] W. Li, B. Song, and A. Manthiram, "High-voltage positive electrode materials for lithium-ion batteries," *Chemical Society Reviews*, vol. 46, no. 10, pp. 3006–3059, 2017.
- [8] M. Kempaiah Devaraju, Q. Duc Truong, H. Hyodo, Y. Sasaki, and I. Honma, "Synthesis, characterization and observation of antisite defects in LiNiPO_4 nanomaterials," *Scientific Reports*, vol. 5, no. 1, article 11041, 2015.
- [9] Z. Zhang, L. Hu, H. Wu et al., "Fluorinated electrolytes for 5 V lithium-ion battery chemistry," *Energy & Environmental Science*, vol. 6, no. 6, pp. 1806–1810, 2013.
- [10] M. Xu, L. Zhou, Y. Dong, Y. Chen, A. Garsuch, and B. L. Lucht, "Improving the performance of graphite/ $\text{LiNi}_{0.5}\text{Mn}_{1.5}\text{O}_4$ cells at high voltage and elevated temperature with added lithium Bis(oxalato) borate (LiBOB)," *Journal of The Electrochemical Society*, vol. 160, no. 11, pp. A2005–A2013, 2013.
- [11] K. Amine, H. Tukamoto, H. Yasuda, and Y. Fujita, "Preparation and electrochemical investigation of $\text{LiMn}_{2-x}\text{Me}_x\text{O}_4$ (Me: Ni, Fe, and $x = 0.5, 1$) cathode materials for secondary lithium batteries," *Journal of Power Sources*, vol. 68, no. 2, pp. 604–608, 1997.
- [12] Q. Zhong, A. Bonakdarpour, M. Zhang, Y. Gao, and J. R. Dahn, "Synthesis and electrochemistry of $\text{LiNi}_x\text{Mn}_{2-x}\text{O}_4$," *Journal of The Electrochemical Society*, vol. 144, no. 1, pp. 205–213, 1997.
- [13] S. J. Lee, J.-G. Han, I. Park et al., "Effect of lithium bis(oxalato) borate additive on electrochemical performance of $\text{Li}_{1.17}\text{Ni}_{0.17}\text{Mn}_{0.5}\text{Co}_{0.17}\text{O}_2$ cathodes for lithium-ion batteries,"

- Journal of The Electrochemical Society*, vol. 161, no. 14, pp. A2012–A2019, 2014.
- [14] A. M. Haregewoin, A. S. Wotango, and B.-J. Hwang, “Electrolyte additives for lithium ion battery electrodes: progress and perspectives,” *Energy Environ. Sci.*, vol. 9, no. 6, pp. 1955–1988, 2016.
- [15] L. Yang, B. Ravdel, and B. L. Lucht, “Electrolyte reactions with the surface of high voltage $\text{LiNi}_{0.5}\text{Mn}_{1.5}\text{O}_4$ cathodes for lithium-ion batteries,” *Electrochemical and Solid-State Letters*, vol. 13, no. 8, pp. A95–A97, 2010.
- [16] A. Von Cresce and K. Xu, “Electrolyte additive in support of 5 v Li ion chemistry,” *Journal of The Electrochemical Society*, vol. 158, no. 3, pp. A337–A342, 2011.
- [17] L. Yang, T. Markmaitree, and B. L. Lucht, “Inorganic additives for passivation of high voltage cathode materials,” *Journal of Power Sources*, vol. 196, no. 4, pp. 2251–2254, 2011.
- [18] K. Xu, “Electrolytes and interphases in Li-ion batteries and beyond,” *Chemical Reviews*, vol. 114, no. 23, pp. 11503–11618, 2014.
- [19] V. Aravindan, J. Gnanaraj, S. Madhavi, and H. Liu, “Lithium-Ion Conducting Electrolyte Salts for Lithium Batteries,” *Chemistry - A European Journal*, vol. 17, no. 51, pp. 14326–14346, 2011.
- [20] M. R. Laskar, D. H. K. Jackson, Y. Guan et al., “Atomic layer deposition of $\text{Al}_2\text{O}_3\text{-Ga}_2\text{O}_3$ alloy coatings for $\text{Li}[\text{Ni}_{0.5}\text{Mn}_{0.3}\text{Co}_{0.2}] \text{O}_2$ cathode to improve rate performance in Li-Ion battery,” *ACS Applied Materials & Interfaces*, vol. 8, no. 16, pp. 10572–10580, 2016.
- [21] J. Liu and A. Manthiram, “Improved electrochemical performance of the 5 V spinel cathode $\text{LiMn}_{1.5}\text{Ni}_{0.42}\text{Zn}_{0.08}\text{O}_4$ by surface modification,” *Journal of The Electrochemical Society*, vol. 156, no. 1, pp. A66–A72, 2009.
- [22] N. Loeffler, G. T. Kim, F. Mueller et al., “In situ coating of li $[\text{Ni}_{0.33}\text{Mn}_{0.33}\text{Co}_{0.33}] \text{O}_2$ particles to enable aqueous electrode processing,” *ChemSusChem*, vol. 9, no. 10, pp. 1112–1117, 2016.
- [23] A. Kazzazi, D. Bresser, A. Birrozzi, J. Von Zamory, M. Hekmatfar, and S. Passerini, “Comparative analysis of aqueous binders for high-energy li-rich NMC as a Lithium-Ion cathode and the impact of adding phosphoric acid,” *ACS Applied Materials & Interfaces*, vol. 10, no. 20, pp. 17214–17222, 2018.
- [24] M. Kuenzel, D. Bresser, T. Diemant et al., “Complementary strategies toward the aqueous processing of high-voltage $\text{LiNi}_{0.5}\text{Mn}_{1.5}\text{O}_4$ lithium-ion cathodes,” *ChemSusChem*, vol. 11, no. 3, pp. 562–573, 2018.
- [25] R. S. Arumugam, L. Ma, J. Li, X. Xia, J. M. Paulsen, and J. R. Dahn, “Special synergy between electrolyte additives and positive electrode surface coating to enhance the performance of $\text{Li}[\text{Ni}_{0.6}\text{Mn}_{0.2}\text{Co}_{0.2}] \text{O}_2/\text{graphite}$ cells,” *Journal of The Electrochemical Society*, vol. 163, no. 13, pp. A2531–A2538, 2016.
- [26] K. Xu, B. Deveney, K. Nechev, Y. Lam, and T. R. Jow, “Evaluating liBOB/lactone electrolytes in large-format lithium-ion cells based on nickelate and iron phosphate,” *Journal of The Electrochemical Society*, vol. 155, no. 12, pp. A959–A964, 2008.
- [27] D. Aurbach and A. Zaban, “Impedance spectroscopy of lithium electrodes: part I. general behavior in propylene carbonate solutions and the correlation to surface chemistry and cycling efficiency,” *Journal of Electroanalytical Chemistry*, vol. 348, no. 1-2, pp. 155–179, 1993.
- [28] W. Li and B. L. Lucht, “Lithium-ion batteries: thermal reactions of electrolyte with the surface of metal oxide cathode particles,” *Journal of The Electrochemical Society*, vol. 153, no. 8, pp. A1617–A1625, 2006.
- [29] M. Nie, D. Chalasani, D. P. Abraham, Y. Chen, A. Bose, and B. L. Lucht, “Lithium ion battery graphite solid electrolyte interphase revealed by microscopy and spectroscopy,” *The Journal of Physical Chemistry C*, vol. 117, no. 3, pp. 1257–1267, 2013.
- [30] D. Lu, M. Xu, L. Zhou, A. Garsuch, and B. L. Lucht, “Failure mechanism of graphite/ $\text{LiNi}_{0.5}\text{Mn}_{1.5}\text{O}_4$ cells at high voltage and elevated temperature,” *Journal of The Electrochemical Society*, vol. 160, no. 5, pp. A3138–A3143, 2013.



Hindawi

Submit your manuscripts at
www.hindawi.com

